CHAPTER 6

Development of an Overlay Design Model for Service Life Prediction against Reflective Cracking

6.1 ABSTRACT

Although reflection of cracking is the major mode of failure in rehabilitated pavement structures, due to its complexity it seldom has been considered in the overlay design process. This chapter discusses the development of an overlay design procedure that will predict the service life of rehabilitated flexible pavement structures against reflective cracking with and without steel reinforcement. Two simple linear regression equations, which were developed based on the results of three-dimensional (3D) finite element (FE) models, are incorporated into a general design framework. These equations consider a controlling set of variables that can provide an adequate description of the pavement performance against reflective cracking: thickness of the overlay, modulus of the overlay's resilience, thickness of the existing hot-mix asphalt (HMA) layers and their effective resilient modulus, thickness of the existing base and its modulus of elasticity, and the elastic modulus of the subgrade. Shift factors were used to account for the differences between simulation and field conditions. Using the Odemark method, the developed regression models can be expanded easily to cover a wide variety of flexible pavement structures. An example is presented to demonstrate the use of the developed design equation in a routine overlay. Finally, long-term field evaluation and adjustment of the developed models are recommended.

6.2 INTRODUCTION

Hot-mix asphalt (HMA) overlays are typically applied to existing flexible and rigid pavements when the structural or functional conditions of the pavement have reached an unacceptable level of service. Reflection cracks caused by the continuous movement of existing joints or cracks in the existing pavements long have been considered a major challenge during pavement rehabilitation, particularly because of the prohibitively high costs with which they are associated.

As the need grows for new rehabilitation methodologies to improve the performance of HMA overlays, interlayer systems offer a feasible solution to the problem when the proper product is used correctly. Until recently, the general belief among pavement engineers was that even when a new technique is effective in delaying reflective cracking, the cost should be equivalent to that of repair (Hughes et al. 1973; Chen and Frederick 1992; Buttlar et al. 2000). As reflection cracking may develop in HMA overlays after a short period of time (as early as a few months, in some cases [Chen and Frederick 1992]) this opinion appears misleading. To validate and quantify the effectiveness of interlayer systems, we must thoroughly understand the contributing mechanism, which could require incorporating into existing and new pavement designs promising new rehabilitation methodologies.

Pavement engineers increasingly recognize that, despite the complexity of pavement systems (especially when reflective cracking is considered), an ideal design tool should be based on well-established engineering theories. The final design approach should be simple but might not be empirical. This chapter presents the formulation of a design scheme, with and without steel reinforcement that considers reflective cracking as the controlling failure mechanism. To formulate the proposed design equations, finite element technique and fracture mechanics principles were used in combination with actual stress and strain measurements at the Virginia Smart Road. While background related to reflective cracking was presented in chapters 3 and 5, the following section covers a brief overview of current flexible pavement design methods.

6.3 BACKGROUND

6.3.1 New Construction Pavement Design

Flexible pavement design consists of two major steps: the design of the paving mixture and the structural design of the pavement layers. The structural design of such pavements depends on many factors, but not all are considered in the creation process due to the uncertainty of their effects on performance. Figure 6-1 presents a schematic of the different pavement design approaches. Accordingly, pavement design models may fall into three major categories (Rauhut 1987):

- **Empirical design method.** This approach consists of a mathematical relationship (or a series of monographs) derived from in-service roads or full-scale experimental facility without any theoretical support for the suggested design method. The major advantages of this method are its simplicity and, since it requires limited testing, its low cost. The major disadvantage of is that they are difficult to use in regions where field conditions are different from those used during model development. The level of reliability achieved by these methods is very low, and pavement performance is unknown.

- **Mechanistic-Empirical design method.** This method is developed based on a combination of field data and mechanistic models. These design methods possess three major advantages: an improved level of design reliability, the ability to predict specific types of distresses, and the possibility of being adapted to different field conditions. Their major disadvantages are that they are usually based on a single set of conditions (subgrade, environmental, etc.) and their performance must be evaluated for a short period of time using accelerated loading testing.

- **Mechanistic design method.** This approach is based on the assumption that pavement can be modeled as a multi-layer elastic or viscoelastic structure (AASHTO 1993).

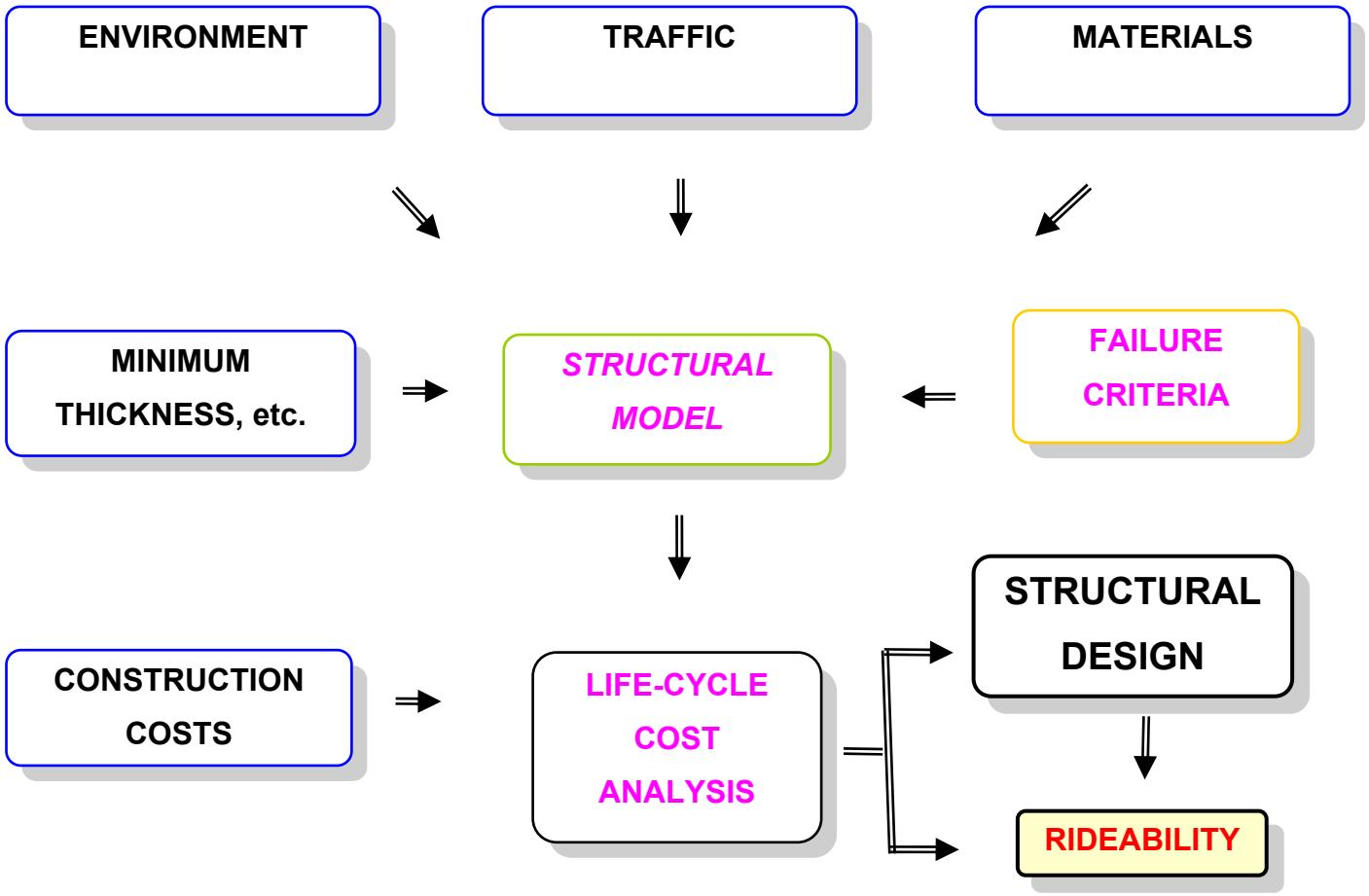

Figure 6-1. Pavement Design Process

From this formulation, it is possible to calculate stresses, strains and deflections at any point within the pavement. Then, using mechanistic models, the calculated straining actions are directly related to pavement performance. This model still requires calibration based on field and/or laboratory observations, but its major advantages are an improved level of design reliability, a clearer understanding of and ability to predict different pavement distresses, and a better allocation of available funds based on the predicted level of performance. Its major disadvantages are a high level of design complexity and an extensive period of laboratory investigation for input parameters.

6.3.2 Flexible Pavement Rehabilitation

When compared to regular flexible pavement design, most of the overlay design procedures are classified as mechanistic in nature. In most approaches to them, mechanistic models are used to relate calculated straining actions to pavement performance. Pavement deflections, condition surveys, and traffic estimate are required as design inputs. This procedure consists of several steps. First, analysis sections are established based on the condition surveys and deflection measurements. Material characterization is then required based on laboratory testing or a back calculation procedure. Using traffic information and material properties adjusted for loading and seasonal variations, critical straining actions are determined using the layered elastic theory. The calculated strains help determine the number of additional load applications that must be applied to the existing pavement for it to resist such critical distresses as fatigue damage, rutting, and thermal cracking-. If an overlay is required, it must be designed to resist potential distress modes. Most of the overlay design approaches propose an increase in pavement fatigue and rutting service life (Pierce et al. 1993; Bayomy et al. 1996). Although reflective cracking is the common failure mechanism in rehabilitated pavements, because of its complexity it is rarely considered in the original overlay design.

A review of the literature indicates no existing design method that is directly applicable to reinforced flexible pavement structures. Moreover, as indicated in Chapter 4, due to the nature of the interlayer system, simulating steel reinforcement in the layered elastic theory may not be appropriate. Therefore, FEM was adopted in this study to achieve a higher level of accuracy and confidence in the results. Results of the analysis were then used to develop a simple design model.

6.4 DESIGN FRAMEWORK

The developed design model is valid only for rehabilitation of flexible pavement structures in which reflective cracking is the failure mechanism. Although not considered in this study, other modules may be added to account for other failure mechanisms and other types of pavement structures (e.g. rigid and composite pavements). A general framework for the developed design method is illustrated in Figure 6-2. The process itself consists of the following steps:

1. **Establish the Structural Design and Capacity of the Existing Pavement Structure.** This step, which can be accomplished using a regular back calculation procedure, consists of first obtaining the surface deflection using a Falling Weight Deflectometer (FWD) and predicting the layer thicknesses and moduli based on equating the measured and calculated deflections. Back calculation software (e.g. MICHBACK, ELMOD, MODULUS, etc.) can be used to match the measured deflections to the calculated ones by iteratively changing the layer moduli and thicknesses. This approach does not offer a unique solution to the problem, so when the number of layers increases significantly, a more sophisticated backcalculation procedure (e.g. FEM presented in Chapter 4) could be required. In fact, most back calculation software programs can handle only four to five pavement layers.

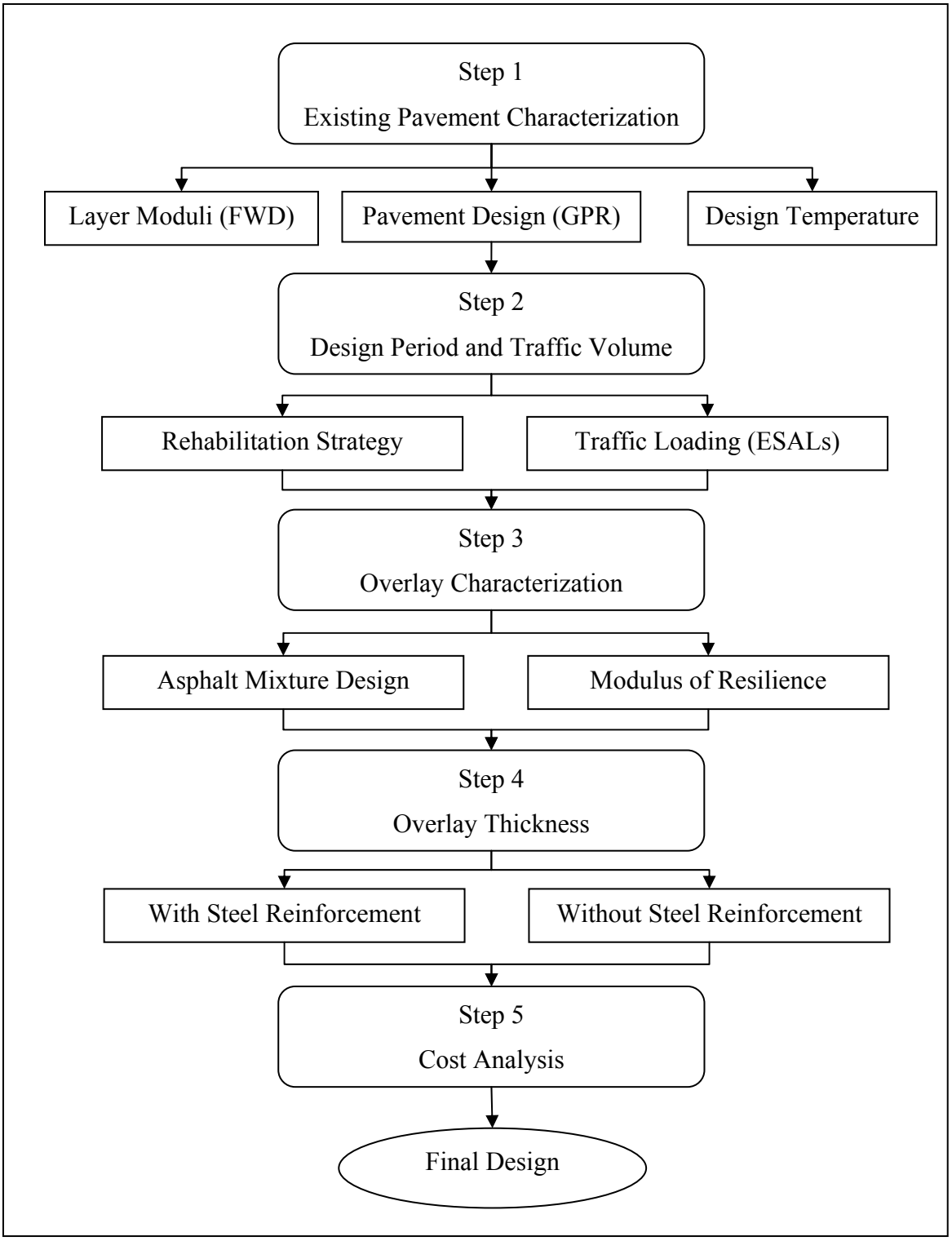

Figure 6-2. Overlay Design Framework

It should be noted, however, that the computed moduli must be adjusted to the design temperature (in the case of this study, 25°C). Several temperature correction models were recently developed to adjust measured deflections to a reference temperature (Kim et al. 1995). Coring or nondestructive techniques (e.g. ground penetrating radar [GPR]) also could be required to accurately determine the structural design of the pavement structure.

2. **Characterize the Selected Overlay Asphalt Mixture Properties.** This step can be accomplished - based on the mix design selected in the laboratory for the overlay. For example, the SuperPave design approach could require several trial mixtures (Roberts et al. 1996). Although SuperPave does not do so, the proposed design method requires characterizing the expected modulus of resilience (M_r) for the overlay at the selected design temperature.

3. **Establish the Traffic Loading and Volume for the Design Period.** Since the pavement will be subject to multiple wheels loading and frequency, the expected traffic is converted to the standard equivalent single axle load (ESAL). Introduced by the AASHO Road Test, this concept converts the damage induced by a specific axle to the equivalent damage induced by a standard 80-kN single-axle load. In this study, the adopted loading configuration consisted of the steering axle used during vehicular testing, a configuration selected for several reasons. First, previous studies have shown that the front is the most detrimental of all axles (Huhtala 1988; Al-Qadi et al. 2002). During vehicular testing, as compared to tandem and tridem ones, this axle also provided the most accurate and reliable instrument responses. This configuration allowed the use of symmetry in loading, which helped significantly reduce computational time. This configuration results in a total load of 58-kN over a single axle with single tire (see Figure 6-3).

Figure 6-3. Equivalency between the Standard Axle and the Steering Axle

The equivalent axle load factor (EALF) for this configuration relative to the standard 80-kN single axle load (W_{t18}) was computed as follows (Huang 1993):

$$EALF = \left(\frac{\varepsilon_x}{\varepsilon_{18}} \right)^4 \tag{6.1}$$

where

EALF = equivalent axle load factor (computed as 1.3378 for a typical overlay design);

ε_x = tensile strain at the bottom of HMA due to the steering axle; and

ε_{18} = tensile strain at the bottom of the HMA due to the standard 80-kN axle load.

The above equation is based on the fourth power law, which was introduced in the findings of the AASHO road test (AASHTO 1972). This relation assumes that both the standard axle and the axle of interest have the same contact pressure but different contact radius. It considers that the damage induced by a given axle is equivalent to the damage induced by the standard axle raised to the fourth power.

6.5 DEVELOPMENT OF DESIGN EQUATIONS

The developed FE codes represent a variety of four-layer systems encountered regularly in typical flexible pavement overlay applications. A partial factory design was developed to include three levels of overlay thickness, three levels of overlay moduli, three levels of HMA thickness, three levels of HMA moduli, three levels of base thickness, two levels of base moduli, and two levels of subgrade moduli; these levels are presented in Table 6-1. A total of 432 different pavement designs were analyzed to develop the suggested design equation. The general layout of an existing pavement structure consists of a cracked HMA layer, a base layer, on top of a subgrade. A HMA overlay is applied to the cracked HMA in variable thicknesses. Each pavement design consists of six to 12 different runs covering different crack locations, reinforced or unreinforced cases, and overlay thickness. Each run required from approximately one to three hours on the college-based super computer known as the 'crunch system'. The assumptions used in these models were presented in Chapter 5.

Omitting the ultimate failure stage, the reflection of a crack to the surface is divided into two distinct phases: crack initiation and crack propagation. Assuming that global instability is reached when the crack front is 12.7 mm from the pavement surface, the total number of cycles before a crack reflects to the surface is defined as follows:

$$N_{total} = N_{initiation} + N_{propagation} \tag{6.2}$$

where

N_{total} = total number of cycles before the crack reach 12.7mm from the surface of the overlay;

$N_{initiation}$ = number of cycles for crack initiation at the bottom of the overlay; and

$N_{propagation}$ = number of cycles for the crack to propagate from the bottom of the overlay to 12.7mm from the surface of the overlay.

Table 6-1. Overview of Investigated Cases

Overlay Thickness (mm)	Overlay Modulus (MPa)	HMA Thickness (mm)	HMA Modulus (MPa)	Base Thickness (mm)	Base Modulus (MPa)	Subgrade Modulus (MPa)
50	3450 (0.25)	100	1725 (0.30)	150	205 (0.35)	40 (0.40)
100	4480 (0.25)	150	2065 (0.30)	300	410 (0.35)	135 (0.40)
150	5510 (0.25)	200	2415 (0.30)	600		

* Poisson's ratio is presented in parenthesis.

Based on the entire set of analytical results, a regression model was developed to predict the number of cycles as a function of the significant variables for the reinforced and unreinforced cases. The total number of cycles, which varies over several orders of magnitude, often results in an excessive accumulation of error components and an overflow in computations. To avoid these problems, the modeling was conducted in the logarithmic domain. To illustrate the convenience of manipulating the number of cycles in the logarithmic domain, consider the comparison between the following cases:

- Assume that the measured number of cycles for one of the design is 1.0E06 versus a predicted number of cycles of 1.3E06. The error in this prediction is 3.0E05 (30% deviation from the measured values). Consider now that the measured number of cycles is 6.0E03 and the predicted number of cycles is 1.0E04. The error in this case is 4.0E03, corresponding to an accuracy of 40%. The total error component for these two cases is 3.04E05, with 98.7% attributed to the first case and 1.3% attributed to the second case. Although the model provided a better estimation in the first case, most of the weight in the total error component also occurred here. It also appears that the total number of errors could indeed be very large, which may result in an unacceptable loss of accuracy.

- In the logarithmic domain, the error in the first case is 5.48, and the error in the second case is 3.60. In this case, the total error component is 9.08, with 60.3% attributed to the first case and 39.7% attributed to the second case. The total error component would also be much smaller in magnitude than in the first case, indicating a more accurate handling of the problem.

The suggested simple regression model has the following form:

$$\text{Log } W_{t80} = aH_{overlay} + bE_{overlay} + cH_{HMA} + dE_{HMA} + eH_{base} + fE_{base} + gE_{subgrade} \quad (6.3)$$

where

W_{t80} = total number of 80-kN single-axle load applications;

a, b, c, d, e, f, and g = regression constants;

$H_{overlay}$ = thickness of HMA overlay (mm);

$E_{overlay}$ = modulus of resilience of HMA overlay (MPa);

H_{HMA} = thickness of existing HMA layer (mm);

E_{HMA} = modulus of resilience of existing HMA layer (MPa);

H_{base} = thickness of base layer (mm);

E_{base} = modulus of resilience of base layer (MPa); and

$E_{subgrade}$ = modulus of resilience of subgrade (MPa).

The interaction between the different variables was also considered, but was found to be statistically insignificant.

6.5.1 Shift Factors

Unless specific shift factors are used to adjust for differences between simulation and field conditions, results from the developed models are not directly applicable to the design of layered pavement systems. Due to differences between laboratory and field conditions, highway

pavements were found to sustain load applications from 10 to 100 times greater than the number of cycles estimated by the laboratory tests (Castell et al. 2000). Within the context of this study, an effort was made to approach field conditions through the use of field-measured stresses for simulating vehicular loading. Therefore, discrepancies between the service life predicted by the design model and the actual pavement service life can be attributed to the following factors:

- Healing of bituminous materials in rest periods between load pulses. This factor represents recovering HMA damage in asphalt mixtures between applications of successive loading. For a typical HMA, previous studies reported a shift factor for healing of up to 20 (Read 2000). The healing process is attributed to two major mechanisms. The first process involves relaxation of the material during rest periods, by which some of its residual strain is lost (Al-Balbissi and Little 1990). The second mechanism gives the material time to heal from the damage. During this process, the size of the plastic zone ahead of the crack tip is reduced, and after the load is removed partial crack closure could occur due to atomic forces between the particles of the material. Based on the reviewed literature, a shift factor of three was assumed (Al-Balbissi and Little 1990; Kim et al. 1997).
- Distribution of load applications in the wander area. This factor addresses the fact that not all vehicles will pass directly on top of the crack; therefore, they will not contribute equally to its initiation and propagation. In reality, vehicles wander between the boundaries of the traffic lane (COST 334 2001). This factor was previously researched at Virginia Tech (Nassar 2001). It was found that the traffic wander can be assumed to follow a normal distribution, with a required shift factor of between 1.6 and 2.7 depending on the standard deviation of the distribution. In this study, a shift factor of two was assumed for traffic wander around the cracked region.
- Other factors such as crack propagation time and inadequacies of pavement models do not play a major role in this study. A shift factor of 1.5 was selected to adjust for the number of cycles estimated for crack initiation (difference in state of stresses between laboratory testing and field conditions). This shift factor agrees with the findings of Nassar (2001), who reported a shift factor of between 1.3 and 5.8 to correct for the state of stresses. While the previous factor is only applied to the crack initiation phase, the shift factors for traffic wander and healing are

applied equally to both crack initiation and propagation phases. Considering the proposed shifting, the final overlay design model is defined as follows:

$$N_{total} = SF_W \times SF_H \times [SF_S \times N_{initiation} + N_{propagation}] \quad (6.4)$$

where

SF_S = shift factor for adjustment of state of stresses (selected as 1.5);

SF_W = shift factor for adjustment of the wander area (selected as two); and

SF_H = shift factor for adjustment of the healing (selected as three).

6.5.2 Design Models

Table 6-2 shows FE analysis results for a sample of the considered pavement designs (unreinforced cases). Results of all the considered designs are presented in Appendix D. The table also shows the values of the regression coefficients for fitting the stress intensity factor behavior during the crack propagation phase. The fitted polynomial regression model follows:

$$K = a_1c^2 + a_2c + a_3 \quad (6.5)$$

where

K = stress intensity factor ($MPa.mm^{0.5}$); and

c = crack length (mm).

It may be noticed from Table 6-2 that the degree of the polynomial was sometimes reduced to a lower level to avoid convergence difficulties in the integration. However, the coefficient of determination (R^2) was always greater than 0.90.

Table 6-2. Calculated Number of Cycles for Crack Initiation and Propagation without Reinforcement

ID	$H_{overlay}$ (mm)	$E_{overlay}$ (MPa)	H_{HMA} (mm)	E_{HMA} (MPa)	H_{base} (mm)	E_{base} (MPa)	$E_{subgade}$ (MPa)	$N_{initiation}$	$N_{propagation}$	W_{t80}	Regression Coefficients		
											a_1	a_2	a_3
1	50	3450	100	2065	150	205	40	6.24E+03	2.60E+04	**4.31E+04**	-0.0014	0.0882	5.4396
2	50	4480	100	2065	150	205	40	1.32E+04	3.49E+04	**6.43E+04**	-0.0078	0.1546	6.4121
3	50	5510	100	2065	150	205	40	2.51E+04	4.49E+04	**9.37E+04**	-0.0028	0.1464	7.2736
4	50	3450	100	2065	150	410	40	9.64E+03	3.14E+04	**5.50E+04**	-0.0003	0.0781	5.1730
5	50	3450	150	2065	150	205	40	1.76E+04	4.43E+04	**8.27E+04**	0.0000	0.0750	4.7182
6	50	3450	100	2065	150	205	135	6.55E+03	2.79E+04	**4.61E+04**	-0.0007	0.0826	5.3328
7	50	3450	100	2065	300	205	40	6.91E+03	2.83E+04	**4.71E+04**	-0.0009	0.0834	5.3191
8	50	3450	100	2065	600	205	40	6.85E+03	2.95E+04	**4.86E+04**	-0.0006	0.0811	5.2598
9	50	3450	200	2065	150	205	40	2.47E+04	5.13E+04	**1.02E+05**	0.0000	0.0737	4.5403
10	50	3450	100	2415	150	205	40	8.01E+03	3.84E+04	**6.21E+04**	-0.0020	0.0789	4.9699
11	50	3450	150	2065	300	410	40	1.76E+04	4.92E+04	**8.93E+04**	0.0034	0.0340	4.6650
12	50	3450	200	2065	300	205	40	2.41E+04	5.47E+04	**1.05E+05**	0.0033	0.0321	4.5477
13	100	3450	100	2065	150	205	40	6.10E+04	1.96E+05	**3.43E+05**	0.0249	0.4679	1.7362
14	100	4480	100	2065	150	205	40	1.46E+05	2.67E+05	**5.53E+05**	0.0000	0.7538	1.8346
15	100	5510	100	2065	150	205	40	3.04E+05	3.39E+05	**8.61E+05**	0.0000	0.8259	2.1367
16	100	5510	100	1725	150	205	135	3.36E+05	2.81E+05	**8.26E+05**	0.0000	0.9156	2.2605
17	100	5510	100	2065	150	410	135	5.08E+05	4.45E+05	**1.27E+06**	0.0000	0.8336	1.9428
18	100	3450	100	2065	150	205	135	7.06E+04	2.17E+05	**3.85E+05**	0.0249	0.4679	1.7362

ID	$H_{overlay}$ (mm)	$E_{overlay}$ (MPa)	H_{HMA} (mm)	E_{HMA} (MPa)	H_{base} (mm)	E_{base} (MPa)	$E_{subgade}$ (MPa)	$N_{initiation}$	$N_{propagation}$	W_{t80}	Regression Coefficients		
											a_1	a_2	a_3
19	100	5510	200	2065	150	205	40	1.12E+06	7.21E+05	**2.46E+06**	0.0247	0.4308	1.7184
20	100	5510	150	2065	150	205	40	6.77E+05	5.72E+05	**1.67E+06**	0.0364	0.6273	1.6893
21	100	5510	150	2065	300	205	40	7.40E+05	6.02E+05	**1.80E+06**	0.0000	0.8493	1.7360
22	100	4480	100	2065	300	205	40	1.74E+05	3.00E+05	**6.34E+05**	0.0000	0.8493	1.6995
23	100	4480	100	2065	150	410	40	2.07E+05	3.10E+05	**6.92E+05**	0.0378	0.4879	1.9922
24	100	4480	100	2065	150	410	135	2.42E+05	3.48E+05	**7.91E+05**	0.0375	0.4891	1.9682
25	150	3450	100	2065	150	205	40	1.63E+05	9.20E+06	**1.25E+07**	0.0005	0.0064	1.4125
26	150	3450	100	2065	300	205	40	1.98E+05	1.05E+07	**1.43E+07**	0.0006	0.0045	1.3628
27	150	3450	100	2065	300	205	135	2.14E+05	1.20E+07	**1.63E+07**	0.0005	0.0060	1.3240
28	150	4480	100	2065	150	205	40	4.00E+05	1.31E+07	**1.80E+07**	0.0006	0.0100	1.5948
29	150	5510	100	2065	150	205	40	8.59E+05	1.86E+07	**2.60E+07**	0.0006	0.0102	1.8361
30	150	3450	150	2065	150	205	40	3.53E+05	1.74E+07	**2.38E+07**	0.0005	0.0049	1.2156
31	150	3450	150	2065	300	205	40	3.92E+05	1.93E+07	**2.63E+07**	0.0005	0.0052	1.1817
32	150	5510	200	2065	150	205	40	2.71E+06	4.17E+07	**5.94E+07**	0.0006	0.0137	1.3292
33	150	5510	200	2065	150	410	40	4.15E+06	7.65E+07	**1.08E+08**	0.0005	0.0292	0.9399
34	150	3450	150	2065	150	205	135	3.88E+05	1.93E+07	**2.64E+07**	0.0005	0.0051	1.1818
35	150	3450	150	2065	600	205	40	4.13E+05	2.09E+07	**2.85E+07**	0.0005	0.0053	1.1563
36	150	3450	100	2065	150	410	135	2.75E+05	1.36E+07	**1.85E+07**	0.0005	0.0064	1.2777

An example of the stress intensity factor fitting for different HMA thickness, and a 150mm overlay thickness is shown in Figure 6-4. The coefficients of determination for the three curves are identical and equal to 0.99; the regression coefficients are shown in Table 6-2. It should be noted also that the fitting curves are sufficiently sensitive to reflect the change in HMA thickness, which affects the number of cycles for the crack to propagate when calculated using Paris Law.

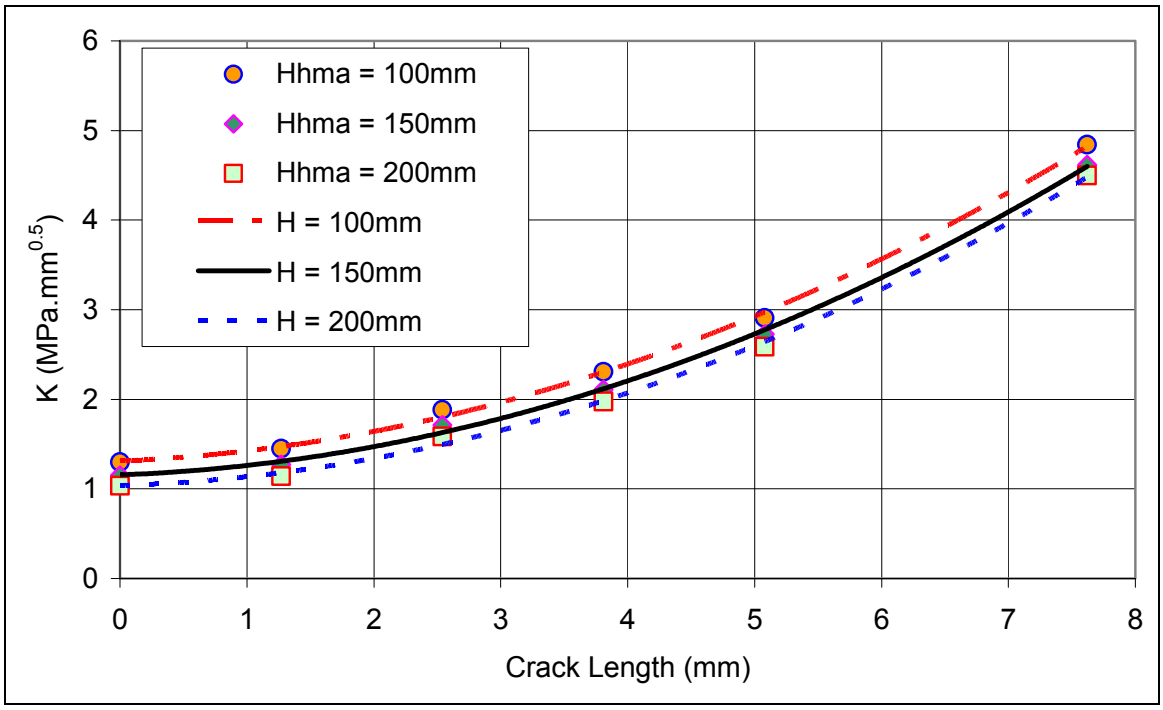

Figure 6-4. Variation of the Stress Intensity Factor for Different HMA Thickness

Considering the amount of shifting for the number of cycles and for an unreinforced overlay, values of the regression coefficients are

$$\text{Log } W_{t80} = \frac{1}{10^4} [255H_{overlay} + 2.08E_{overlay} + 45.3H_{HMA} + 8.73E_{HMA} + 1.34H_{base} + 6.93E_{base} + 1.49E_{subgrade}] \quad (6.6)$$

The considered variables appear to provide an adequate description of the pavement behavior with a root mean square error (RMSE) of only 0.053. As shown in Table 6-3, all considered variables except the subgrade statistically affect the total number of cycles at a level of significance of 0.01%. However, when observing the variation of the total number of cycles with respect to the subgrade strength (see Table 6-2 and Appendix D for all the results), the pavement performance against reflective cracking is slightly improved when the subgrade strength increases. Since this enhancement is relatively small, it is not evident in the logarithmic domain, and is, therefore, not detected statistically.

Table 6-3. Analysis of Variance for the Unreinforced Pavements

Source	DF	Type III SS	Mean Square	F Value	Pr (%) > F
Model	8	----	29.641	10546.4	0.01
$H_{overlay}$	2	224.41	112.205	39922.9	0.01
$E_{overlay}$	1	3.838	3.838	1365.77	0.01
H_{HMA}	1	5.126	5.126	1823.90	0.01
E_{HMA}	1	0.602	0.602	214.35	0.01
H_{base}	1	0.044	0.044	15.83	0.01
E_{base}	1	0.171	0.171	61.03	0.01
$E_{subgrade}$	1	0.007	0.008	2.84	9.32

The coefficient of determination for this equation was 0.99, with a RMSE of 0.03. The overlay thickness is undoubtedly the major factor in dictating the overlay performance against reflective cracking failure, followed by the thickness of the existing HMA layer. It appears that the base thickness and subgrade modulus have the least effect on overlay performance. Figure 6-5 compares the calculated design lives using FE with those predicted using Equation (6.6). Fifteen pavement designs (five of each overlay thickness category) were not included in the development of the design equation. These designs were used to check the accuracy of the model.

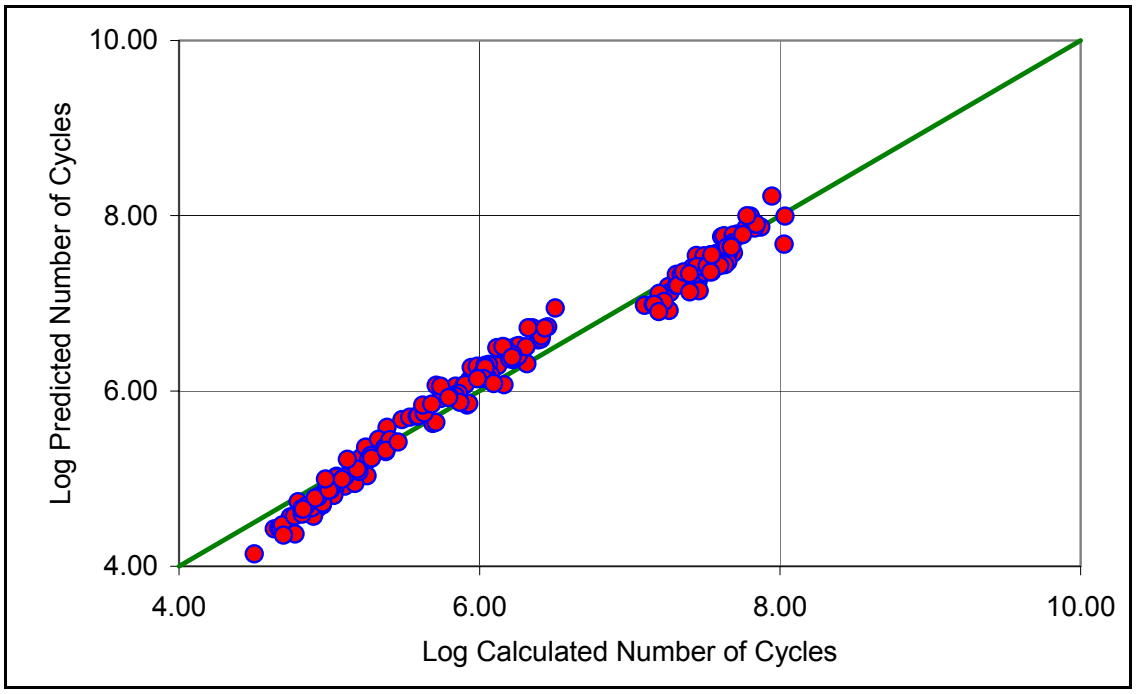

Figure 6-5. Comparison between Calculated and Predicted Number of Cycles (Unreinforced)

Similarly, Table 6-4 illustrates the results of FE analysis for a sample of the reinforced pavement designs and presents the percentage of improvement that results from using steel reinforcement in the crack initiation and propagation phases. Appendix D presents the results for all cases.

Table 6-4. Calculated Number of Cycles for Crack Initiation and Propagation with Reinforcement

ID	$H_{overlay}$ (mm)	$E_{overlay}$ (MPa)	H_{HMA} (mm)	E_{HMA} (MPa)	H_{base} (mm)	E_{base} (MPa)	$E_{subgrade}$ (MPa)	$N_{initiation}$	$N_{propagation}$	W_{t80}	Percentage Improvement (%)		
											Initiation	Propagation	Total
1	50	3450	100	2065	150	205	40	7.04E+03	5.46E+04	**8.25E+04**	12.8%	110.6%	91.6%
2	50	4480	100	2065	150	205	40	1.55E+04	6.49E+04	**1.08E+05**	17.4%	86.2%	67.3%
3	50	5510	100	2065	150	205	40	3.01E+04	7.41E+04	**1.39E+05**	19.9%	65.0%	48.8%
4	50	3450	100	2065	150	410	40	1.10E+04	7.05E+04	**1.09E+05**	14.5%	124.2%	98.5%
5	50	3450	150	2065	150	205	40	2.07E+04	1.11E+05	**1.76E+05**	17.8%	150.7%	113.0%
6	50	3450	100	2065	150	205	135	7.55E+03	6.03E+04	**9.08E+04**	15.3%	116.0%	96.8%
7	50	3450	100	2065	300	205	40	7.86E+03	6.09E+04	**9.21E+04**	13.7%	115.4%	95.5%
8	50	3450	100	2065	600	205	40	7.82E+03	6.46E+04	**9.69E+04**	14.2%	119.2%	99.4%
9	50	3450	200	2065	150	205	40	2.96E+04	1.41E+05	**2.28E+05**	19.7%	174.5%	124.2%
10	50	3450	100	2415	150	205	40	8.57E+03	7.91E+04	**1.17E+05**	7.0%	105.8%	88.7%
11	50	3450	150	2065	300	410	40	2.10E+04	1.26E+05	**1.97E+05**	19.2%	156.7%	120.5%
12	50	3450	200	2065	300	205	40	2.90E+04	1.49E+05	**2.38E+05**	20.2%	171.8%	125.5%
13	100	3450	100	2065	150	205	40	7.79E+04	3.94E+05	**6.32E+05**	27.6%	101.7%	84.1%
14	100	4480	100	2065	150	205	40	1.88E+05	4.42E+05	**8.43E+05**	29.5%	65.1%	52.5%
15	100	5510	100	2065	150	205	40	3.95E+05	5.08E+05	**1.21E+06**	29.8%	49.6%	40.3%
16	100	5510	100	1725	150	205	135	4.61E+05	4.17E+05	**1.17E+06**	37.1%	48.2%	42.1%
17	100	5510	100	2065	150	410	135	6.64E+05	6.77E+05	**1.79E+06**	30.7%	52.3%	40.8%
18	100	3450	100	2065	150	205	135	9.05E+04	3.77E+05	**6.26E+05**	28.2%	73.7%	62.5%

ID	$H_{overlay}$ (mm)	$E_{overlay}$ (MPa)	H_{HMA} (mm)	E_{HMA} (MPa)	H_{base} (mm)	E_{base} (MPa)	$E_{subgrade}$ (MPa)	$N_{initiation}$	$N_{propagation}$	W_{t80}	Percentage Improvement (%)		
											Initiation		
19	100	5510	200	2065	150	205	40	1.48E+06	1.19E+06	**3.57E+06**	45.2%	32.5%	65.0%
20	100	5510	150	2065	150	205	40	8.83E+05	8.32E+05	**2.29E+06**	37.4%	30.5%	45.5%
21	100	5510	150	2065	300	205	40	9.68E+05	8.99E+05	**2.50E+06**	39.1%	30.8%	49.4%
22	100	4480	100	2065	300	205	40	2.27E+05	4.91E+05	**9.60E+05**	51.4%	30.0%	63.9%
23	100	4480	100	2065	150	410	40	2.69E+05	5.18E+05	**1.05E+06**	52.1%	30.1%	66.8%
24	100	4480	100	2065	150	410	135	3.17E+05	5.73E+05	**1.19E+06**	50.7%	30.7%	64.5%
25	150	3450	100	2065	150	205	40	2.12E+05	1.49E+07	**2.03E+07**	30.1%	62.3%	61.8%
26	150	3450	100	2065	300	205	40	2.59E+05	2.18E+07	**2.96E+07**	30.7%	108.2%	106.8%
27	150	3450	100	2065	300	205	135	2.81E+05	2.47E+07	**3.34E+07**	31.0%	105.7%	104.4%
28	150	4480	100	2065	150	205	40	5.25E+05	2.42E+07	**3.31E+07**	31.3%	85.2%	83.6%
29	150	5510	100	2065	150	205	40	1.13E+06	2.92E+07	**4.06E+07**	31.1%	57.5%	56.3%
30	150	3450	150	2065	150	205	40	4.64E+05	3.09E+07	**4.19E+07**	31.4%	77.0%	76.1%
31	150	3450	150	2065	300	205	40	5.18E+05	3.39E+07	**4.60E+07**	32.0%	76.0%	75.2%
32	150	5510	200	2065	150	205	40	3.59E+06	7.13E+07	**1.00E+08**	32.5%	71.0%	68.7%
33	150	5510	200	2065	150	410	40	4.87E+06	2.00E+08	**2.74E+08**	17.3%	161.8%	154.4%
34	150	3450	150	2065	150	205	135	5.12E+05	3.55E+07	**4.82E+07**	32.0%	83.6%	82.6%
35	150	3450	150	2065	600	205	40	5.46E+05	3.71E+07	**5.04E+07**	32.3%	77.9%	77.0%
36	150	3450	100	2065	150	410	135	3.62E+05	2.46E+07	**3.34E+07**	31.6%	81.3%	80.4%

Similarly, Table 6-5 summarizes variance (ANOVA) analysis for the reinforced cases. As shown in this table, the same trend was observed regarding the effects of different variables. The RMSE for the model is 0.0668.

Table 6-5. Analysis of Variance for the Reinforced Cases

Source	DF	Type III SS	Mean Square	F Value	Pr (%) > F
Model	8	----	228.145	6393.40	0.01
$H_{overlay}$	2	215.52	107.763	24159.2	0.01
$E_{overlay}$	1	2.3676	2.367	530.78	0.01
H_{HMA}	1	5.7225	5.7225	1282.92	0.01
E_{HMA}	1	0.4897	0.4897	109.79	0.01
H_{base}	1	0.0604	0.0604	13.54	0.01
E_{base}	1	0.1576	0.1576	35.34	0.01
$E_{subgrade}$	1	0.0179	0.0179	4.01	4.66

The fitted design model for a steel-reinforced pavement structure is the following (R^2 = 0.99):

$$\text{Log } W_{t80} = \frac{1}{10^4} [250H_{overlay} + 1.88E_{overlay} + 50.6H_{HMA} + 9.86E_{HMA} + 1.64H_{base} + 7.46E_{base} + 2.85E_{subgrade}] \quad (6.7)$$

Figure 6-6 compares the calculated design lives using FE with those predicted using Equation 6.7.

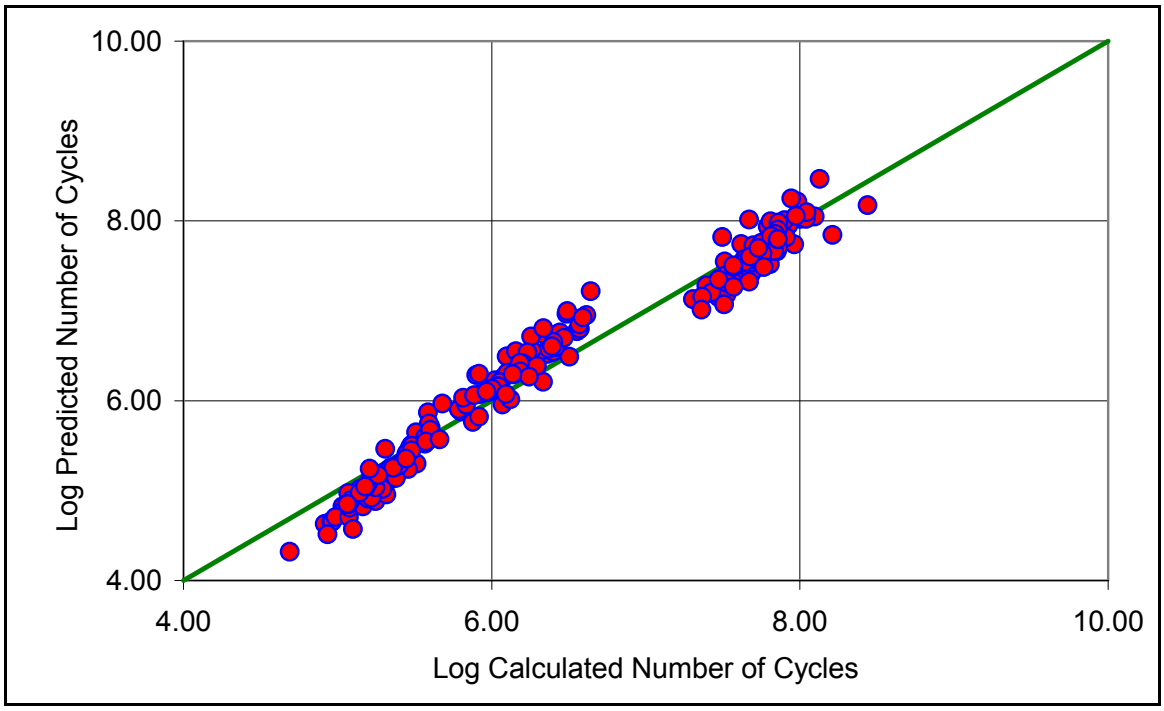

Figure 6-6. Comparison between Calculated and Predicted Number of Cycles (Reinforced)

Although this model was developed based on four-layer pavement structures, it can be extended using Odemark's Method to cover a broader number of cases. Based on the assumption that the straining actions within a layer depend only on the stiffness of that layer, this method allows transforming a layer thickness with a specific stiffness into an equivalent thickness with an arbitrary stiffness. For example, if a subbase is used, it may be converted to an equivalent base thickness as follows (Ullidtz 1987):

$$h_e = h_{sub}\left[\frac{E_{sub}(1-\upsilon_{base}^2)}{E_{base}(1-\upsilon_{sub}^2)}\right]^{1/3} \quad (6.8)$$

where

h_e = equivalent base thickness; and

h_{sub} = original subbase thickness.

This approximation, which is adopted by one of the most used back calculation software programs, ELMOD 4, was found acceptable given two conditions (Ullidtz 1998):

- Moduli decrease with depth , and
- The equivalent thickness of each layer is larger than the radius of the loaded area.

6.5.3 Design Examples

To illustrate the application of the model, the following example is presented. Assume a pavement structure consists of a 150mm HMA layer (E_{HMA}=2415MPa, ν=0.25), 150mm base layer (E_{base}=275MPa, ν=0.35), 300mm subbase layer ($E_{subbase}$=135MPa, ν=0.35), on top of a subgrade ($E_{subgrade}$=135MPa, ν=0.40). Using Odemark's Method, the subbase layer is transformed to an equivalent base layer, resulting in a total base thickness of 385mm. The designer estimates a total accumulative traffic (80-kN repetitions) of $1.2x10^6$ over the service life of the overlay.

Using Equation 6.6, to sustain the estimated traffic the required overlay thickness is 75mm (E=5510MPa, ν=0.25). If steel reinforcement is used, a 75-mm overlay would perform for a total accumulative traffic of $2.28x10^6$, indicating a 90 % improvement in the overlay service against reflective cracking. Depending on fund availability, to maximize the benefit-cost ratio, the designer can then decide to use a multi-stage construction strategy, a reinforcing interlayer system, or any other rehabilitation alternative.

6.6 SUMMARY

A simple design model was developed to predict the service life of an overlay with and without steel reinforcement against reflective cracking. The developed model utilizes a large number of 3D FE models that account for both crack initiation and propagation phases. Using the Odemark Method, the developed model can be expanded to cover flexible pavement systems with more than three layers. The developed model can

effectively to predict the number of cycles to failure against reflective cracking for rehabilitated flexible pavement structures. The steel netting interlayer is found to reinforce pavement structures. However, the extent of improvement is a function of the pavement layer thicknesses and properties. Validation and long-term field evaluation of the proposed model are recommended.

As with any pavement rehabilitation strategy, the use of steel reinforcement must be based on a detailed design and cost analysis. Regardless of the use of a steel reinforcement interlayer system, the overlay thickness remains an important factor in the performance of pavement against reflective cracking failure.

6.7 REFERENCES

AASHTO. (1972). *Interim guide for design of pavement structures*, American Association of State Highway and Transportation Officials, Washington, D.C.

AASHTO. (1993). *Guide for design of pavement structures*, American Association of State Highway and Transportation Officials, Washington, D.C.

Al-Balbissi, A., and Little, D. N. (1990). "Effect of fracture healing on laboratory-to-field shift factor." *Transportation Research Record 1286*, Transportation Research Board, Washington, D.C., 173-183.

Bayomy, F. M., Al-Kandari, F. A., and Smith, R. (1996). "Mechanically based flexible overlay design system for Idaho." *Transportation Research Record 1543*, Transportation Research Board, Washington, D.C., 10-19.

Buttlar, W. G., Bozkurt, D., and Dempsey, B. J. (2000). "Cost-effectiveness of paving fabrics used to control reflective cracking." *Transportation Research Record 1730*, Transportation Research Board, Washington, D.C., 139-149.

Castell, M. A., Ingraffea, A. R., and Irwin, L. H. (2000). "Fatigue crack growth in pavements." *Journal of Transportation Engineering*, American Society of Civil Engineering, 283-290.

Chen, H. J., and Frederick, D. A. (1992). "Interlayers on flexible pavements." *Transportation Research Record 1374*, Transportation Research Board, Washington, D.C.

COST 334. (2001). "Effects of wide single tyres and dual tyres." Final Report of the Action (Version 29), European Cooperation in the field of Scientific and Technical Research.

Finn, F. N., and Monismith, C. L. (1984). "Asphalt overlay design procedures." NCHRP 116, Transportation Research Board, Washington, D.C.

Huang, Y. H. (1993). *Pavement analysis and design,* 1st ed. Prentice-Hall, NJ.

Huges, C. S., and McGhee, K. H. (1973). "Results of reflective crack questionnaire survey." Report No. VHRC 72-R25, Virginia Highway Research Council, Charlottesville, VA.

Huhtala, M. (1988). "The effects of different trucks on road pavements." *Proc., International Symposium on Heavy Vehicle Weights and Dimensions*, Roads and Transportation Association of Canada, Kelowna, BC, Canada, 151-159.

Kim, Y. R., Hibbs, B. O., and Lee, Y-C. (1995). "Temperature correction of deflections and backcalculated asphalt concrete moduli." *Transportation Research Record 1473*, Transportation Research Board, Washington, D.C., 55-62.

Kim, Y. R., Lee, H.-J., Kim, Y., and Little, D. N. (1997). "Mechanistic evaluation of fatigue damage growth and healing of asphalt concrete: laboratory and field experiments." *Proc., Eight International Conference on Asphalt Pavements*, Seattle, Washington, 1090-1107.

Nassar, W. M. (2001). "Utilization of instrument response of SuperPave™ mixes at the Virginia Smart Road to calibrate laboratory developed fatigue equation." PhD Dissertation, Virginia Tech, Blacksburg, VA.

Pierce, L. M., Jackson, N. C., and Mahoney, J. P. (1993). "Development and implementation of a mechanistic, empirically-based overlay design procedure for flexible pavements." *Transportation Research Record 1388*, Transportation Research Board, Washington, D.C., 120-129.

Rauhut, J. B., and Gendell, D. S. "Proposed development of pavement performance prediction models from SHTP/LTTP data." *Proc., Second North American Conference on Managing Pavements*, 2, Toronto, Canada, 2.21-2.37.

Read, J. M. (2000). "New method for measuring crack propagation in asphalts." *International Journal of Pavement Engineering*, Vol. I, No. 1, 15-34.

Roberts, F.L., Kandhal, P.S., Brown, E.R., Lee, D. and Kennedy, T.W. (1996). "Hot mix asphalt materials, mixture design, and construction." 2nd ed., NAPA Education Foundation, Lanham, MD.

Ullidtz, P. (1987). *Pavement analysis,* Elsevier Science, New York, NY.

Ullidtz, P. (1998). *Modelling flexible pavement response and performance,* 1st ed., Polyteknisk Forlag, Denmark.